

The extraction of $\phi - N$ total cross section from $d(\gamma, pK^+K^-)n$

X. Qian,¹ W. Chen,¹ H. Gao,¹ K. Hicks,² K. Kramer,¹ J.M. Laget,^{3,4} T. Mibe,² S. Stepanyan,⁴ D.J. Tedeschi,⁵ W. Xu,⁶ K.P. Adhikari,³² M. Amaryan,³² M. Anghinolfi,²³ H. Baghdasaryan,³⁹ J. Ball,³ M. Battaglieri,²³ V. Batourine,⁴ I. Bedlinskiy,²⁶ M. Bellis,¹¹ A.S. Biselli,^{16,33} C. Bookwalter,¹⁸ D. Branford,¹⁵ W.J. Briscoe,¹⁹ W.K. Brooks,^{38,4} V.D. Burkert,⁴ S.L. Careccia,³² D.S. Carman,⁴ P.L. Cole,^{21,4} P. Collins,⁸ V. Crede,¹⁸ A. D'Angelo,^{24,35} A. Daniel,² N. Dashyan,⁴¹ R. De Vita,²³ E. De Sanctis,²² A. Deur,⁴ B. Dey,¹¹ S. Dhamija,¹⁷ R. Dickson,¹¹ C. Djalali,⁵ G.E. Dodge,³² D. Doughty,^{13,4} R. Dupre,⁷ P. Eugenio,¹⁸ G. Fedotov,³⁶ S. Fegan,²⁰ R. Fersch,^{40,*} A. Fradi,²⁵ M.Y. Gabrielyan,¹⁷ G.P. Gilfoyle,³⁴ K.L. Giovanetti,²⁷ F.X. Girod,^{3,†} J.T. Goetz,⁹ W. Gohn,¹⁴ E. Golovatch,^{36,23} R.W. Gothe,⁵ K.A. Griffioen,⁴⁰ M. Guidal,²⁵ L. Guo,^{4,‡} K. Hafdi,⁷ H. Hakobyan,^{38,41} C. Hanretty,¹⁸ N. Hassall,²⁰ D. Heddle,^{13,4} M. Holtrop,³⁰ C.E. Hyde,³² Y. Ilieva,^{5,19} D.G. Ireland,²⁰ B.S. Ishkhanov,²⁹ E.L. Isupov,³⁶ S.S. Jawalkar,⁴⁰ J.R. Johnstone,²⁰ K. Joo,^{14,4} D. Keller,² M. Khandaker,³¹ P. Khetarpal,³³ W. Kim,²⁸ A. Klein,³² F.J. Klein,^{12,4} V. Kubarovsky,⁴ S.V. Kuleshov,^{38,26} V. Kuznetsov,²⁸ K. Livingston,²⁰ H.Y. Lu,⁵ D. Martinez,²¹ M. Mayer,³² M.E. McCracken,¹¹ B. McKinnon,²⁰ C.A. Meyer,¹¹ T. Mineeva,¹⁴ M. Mirazita,²² V. Mokeev,^{36,4} K. Moriya,¹¹ B. Morrison,⁸ E. Munevar,¹⁹ P. Nadel-Turonski,¹² R. Nasseripour,^{5,17,§} C.S. Nepali,³² S. Niccolai,^{25,19} G. Niculescu,²⁷ I. Niculescu,^{27,19} M.R. Niroula,³² M. Osipenko,²³ A.I. Ostrovidov,¹⁸ K. Park,^{5,28,†} S. Park,¹⁸ E. Pasyuk,⁸ S. Anefalos Pereira,²² S. Pisano,²⁵ O. Pogorelko,²⁶ S. Pozdniakov,²⁶ J.W. Price,¹⁰ S. Procureur,³ D. Protopopescu,²⁰ B.A. Raue,^{17,4} G. Ricco,²³ M. Ripani,²³ B.G. Ritchie,⁸ G. Rosner,²⁰ P. Rossi,²² F. Sabatié,³ M.S. Saini,¹⁸ C. Salgado,³¹ D. Schott,¹⁷ R.A. Schumacher,¹¹ H. Seraydaryan,³² Y.G. Sharabian,^{4,41} E.S. Smith,⁴ D.I. Sober,¹² D. Sokhan,¹⁵ I.I. Strakovsky,¹⁹ S. Strauch,^{5,19} M. Taiuti,²³ S. Tkachenko,³² M. Ungaro,¹⁴ M.F. Vineyard,^{37,34} D.P. Watts,^{20,¶} L.B. Weinstein,³² D.P. Weygand,⁴ M. Williams,¹¹ E. Wolin,⁴ M.H. Wood,⁵ L. Zana,³⁰ J. Zhang,³² B. Zhao,^{14,**} and Z.W. Zhao⁵

(The CLAS Collaboration)

¹Duke University, Durham, North Carolina 27708

²Ohio University, Athens, Ohio 45701

³CEA, Centre de Saclay, Irfu/Service de Physique Nucléaire, 91191 Gif-sur-Yvette, France

⁴Thomas Jefferson National Accelerator Facility, Newport News, Virginia 23606

⁵University of South Carolina, Columbia, South Carolina 29208

⁶Massachusetts Institute of Technology, Cambridge, Massachusetts 02139-4307

⁷Argonne National Laboratory

⁸Arizona State University, Tempe, Arizona 85287-1504

⁹University of California at Los Angeles, Los Angeles, California 90095-1547

¹⁰California State University, Dominguez Hills, Carson, CA 90747

¹¹Carnegie Mellon University, Pittsburgh, Pennsylvania 15213

¹²Catholic University of America, Washington, D.C. 20064

¹³Christopher Newport University, Newport News, Virginia 23606

¹⁴University of Connecticut, Storrs, Connecticut 06269

¹⁵Edinburgh University, Edinburgh EH9 3JZ, United Kingdom

¹⁶Fairfield University, Fairfield CT 06824

¹⁷Florida International University, Miami, Florida 33199

¹⁸Florida State University, Tallahassee, Florida 32306

¹⁹The George Washington University, Washington, DC 20052

²⁰University of Glasgow, Glasgow G12 8QQ, United Kingdom

²¹Idaho State University, Pocatello, Idaho 83209

²²INFN, Laboratori Nazionali di Frascati, 00044 Frascati, Italy

²³INFN, Sezione di Genova, 16146 Genova, Italy

²⁴INFN, Sezione di Roma Tor Vergata, 00133 Rome, Italy

²⁵Institut de Physique Nucléaire ORSAY, Orsay, France

²⁶Institute of Theoretical and Experimental Physics, Moscow, 117259, Russia

²⁷James Madison University, Harrisonburg, Virginia 22807

²⁸Kyungpook National University, Daegu 702-701, Republic of Korea

²⁹Moscow State University, Moscow, Russia

³⁰University of New Hampshire, Durham, New Hampshire 03824-3568

³¹Norfolk State University, Norfolk, Virginia 23504

³²Old Dominion University, Norfolk, Virginia 23529

³³Rensselaer Polytechnic Institute, Troy, New York 12180-3590

³⁴University of Richmond, Richmond, Virginia 23173

³⁵Universita' di Roma Tor Vergata, 00133 Rome Italy

³⁶*Skobeltsyn Nuclear Physics Institute, Skobeltsyn Nuclear Physics Institute, 119899 Moscow, Russia*

³⁷*Union College, Schenectady, NY 12308*

³⁸*Universidad Técnica Federico Santa María, Casilla 110-V Valparaíso, Chile*

³⁹*University of Virginia, Charlottesville, Virginia 22901*

⁴⁰*College of William and Mary, Williamsburg, Virginia 23187-8795*

⁴¹*Yerevan Physics Institute, 375036 Yerevan, Armenia*

(Dated: November 19, 2018)

We report on the first measurement of the differential cross section of ϕ -meson photoproduction for the $d(\gamma, pK^+K^-)n$ exclusive reaction channel. The experiment was performed using a tagged-photon beam and the CEBAF Large Acceptance Spectrometer (CLAS) at Jefferson Lab. A combined analysis using data from the $d(\gamma, pK^+K^-)n$ channel and those from a previous publication on coherent ϕ production on the deuteron has been carried out to extract the $\phi - N$ total cross section, $\sigma_{\phi N}$. The extracted $\phi - N$ total cross section favors a value above 20 mb. This value is larger than the value extracted using vector-meson dominance models for ϕ photoproduction on the proton.

PACS numbers: 13.60.Le, 24.85.+p, 25.10.+s, 25.20.-x

Multi-gluon exchange between hadrons, known as Pomeron exchange, is a fundamental process and plays an important role in high-energy interactions. At lower energies, this exchange manifests itself in a QCD van der Waals interaction [1]. Studying multi-gluon exchange at lower energies is challenging because at low energies hadron-hadron interactions are dominated by quark exchange. However, multi-gluon exchange is expected to be dominant in the interaction between two hadrons when they have no common quarks. The ϕ meson is unique in that it is nearly an $s\bar{s}$ state and hence gluon exchange is expected to dominate the $\phi - N$ scattering process.

Direct measurement of the $\phi - N$ cross section is not possible due to lack of ϕ meson beams. An upper limit of $\sigma_{\phi N} \simeq 11$ mb [2] is obtained using the ϕ photoproduction data on the proton and the vector meson dominance (VMD) model [3], which is in agreement with the estimate from the additive quark model [4]. In a geometric interpretation of hadron-proton total cross sections [5], the radius of the ϕ meson r_ϕ can be estimated from the comparison of the total cross sections of $\pi - N$ ($\sigma_{\pi N}$) and $\phi - N$ ($\sigma_{\phi N}$) scattering. The value of $\sigma_{\pi N}$ is ~ 24 mb [5] and the π radius r_π is ~ 0.65 fm [5]. An upper limit of $\sigma_{\phi N} \sim 11$ mb [2] leads to an upper limit value of ~ 0.43 fm for r_ϕ .

However, from the observed A -dependence of nuclear ϕ photoproduction, a larger value of (inelastic $\sigma_{\phi N}^{inelas} \simeq 35$ mb [6], which is part of the total $\sigma_{\phi N}$) is obtained, which suggests a larger r_ϕ value than 0.43 fm. Medium modification of the vector meson properties [7] (such as radius) or channel coupling effects [2] have been proposed to explain the aforementioned difference in the cross section for the ϕ meson. A similar phenomenon has been observed for the J/Ψ meson [8] and the color transparency effect is proposed [9] to explain the observation.

In this paper, we present a determination of $\sigma_{\phi N}$ using the differential cross section of the incoherent ϕ -meson photoproduction from deuterium. This process takes advantage of the rescattering of a ϕ meson from the specta-

tor nucleon. In the reaction $\gamma + d \rightarrow \phi + p + n$, the rescattering process will dominate for the kinematics where both nucleons are energetic. The deuteron is a system of loosely bound nucleons and, hence, nuclear medium effects should not play a significant role in the $\phi - N$ scattering process. In the analysis of incoherent ϕ -meson photoproduction from deuterium, the $\phi - N$ interaction is parametrized as $\frac{d\sigma}{dt} \propto \sigma_{\phi N}^2 \cdot e^{\beta_{\phi N} t}$ [10, 11, 12], where $\beta_{\phi N}$ characterizes the t -dependence of the differential cross section, and t is defined as the four-momentum transfer squared between the photon and the ϕ meson. A χ^2 analysis is performed for both processes ($\gamma + d \rightarrow \phi + d$ as in [13] and $\gamma + d \rightarrow \phi + p + n$) in this paper to constrain the values of $\sigma_{\phi N}$ and $\beta_{\phi N}$.

The rescattering of a ϕ meson off a nucleon in the deuteron was used to study the $\phi - N$ interaction in a recent analysis of CLAS g10 data using coherent ϕ photoproduction, $\gamma + d \rightarrow \phi + d$ [13]. In the coherent ϕ production process, rescattering dominates in the high $|t|$ region. Results of Ref.[13] agree with the VMD prediction (where $\beta_{\phi N}$ is assumed to be the one in the ϕ -meson photoproduction from a nucleon), however, larger $\sigma_{\phi N}$ values showed better agreement with the data if one allowed the slope ($\beta_{\phi N}$) of the t -dependence of the $\phi - N$ scattering process to be different.

The reaction $\gamma(d, \phi p)n$ was measured by detecting kaons from the ϕ -meson decay ($\phi \rightarrow K^+K^-$, branching ratio about 0.5) using the same data set as in Ref. [13]. A tagged-photon beam was generated by a 3.8-GeV electron beam incident on a gold radiator (10^{-4} radiation length). The photon flux was measured by the CLAS photon-tagger system [14]. The data were collected from a 24-cm-long liquid-deuterium target in the CLAS detector [15] at JLab.

Events having the final state $\gamma + d \rightarrow K^+ + K^- + p + X$ were selected using a triple coincidence detection of a proton, a K^+ and, a K^- . Each particle was selected based on particle charge, momentum, and Time-of-Flight (TOF) information. The reaction $d(\gamma, pK^+K^-)n$ was

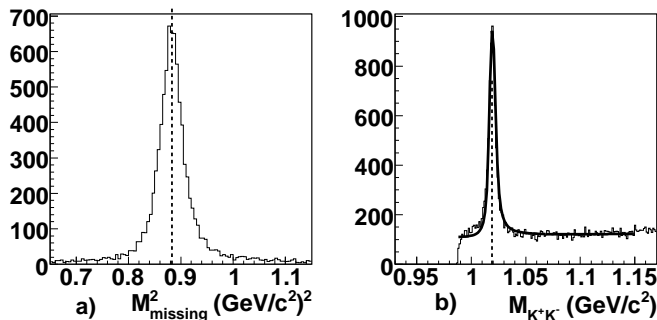


FIG. 1: (a) The missing mass squared distribution; (b) the invariant mass distribution for the K^+K^- for photon energies between 1.65 to 3.59 GeV for the $\gamma + d \rightarrow K^+ + K^- + p + X$ process. Also shown in (b) is a fit using a Breit-Wigner function convoluted with the experimental resolution together with a flat background.

identified in the missing mass squared distribution by the missing neutron shown in Fig. 1a. In the figure, the position of the neutron mass squared is shown by the dotted line. A $\pm 3\sigma$ cut was employed to select the $pK^+K^-(n)$ final state events.

Once the reaction $d(\gamma, pK^+K^-)n$ was identified, the number of ϕ mesons was obtained by subtracting the background under the ϕ peak (invariant mass spectrum of the K^+ and K^-) in the $\pm 3\sigma$ region (see Fig. 1b). The K^+K^- invariant mass distribution was fitted using a Breit-Wigner function convoluted with the experimental resolution, plus a function to model the background in each photon energy and $|t - t_0|$ bin, where t_0 is the minimum t value for a given photon energy. The background shape was assumed to be [13]:

$$\begin{aligned} f(x) &= a\sqrt{x^2 - (2M_K)^2} + b(x^2 - (2M_K)^2) \quad (x > 2M_K) \\ f(x) &= 0 \quad (x < 2M_K), \end{aligned} \quad (1)$$

where x is the invariant mass of the K^+K^- , M_K is the kaon mass, and a and b are fitting parameters. The background was also fitted with a linear shape. The results from fitting these two shapes were compared to estimate the systematic uncertainties due to the subtraction of the background.

A Monte Carlo (MC) [16] simulation of the CLAS detector was carried out to determine the efficiency for the detection of the $\gamma + d \rightarrow p + K^+ + K^-$ reaction. Two event generators were used in two different missing neutron momentum regions. A quasi-free event generator for the $\gamma + p \rightarrow \phi + p$ process in the deuteron was employed for the missing neutron momentum distribution below 0.18 GeV/c, where the agreement between the MC simulation and the data is very good. The deuteron wave function was based on the Bonn potential [17]. The differential cross sections from CLAS [18] for ϕ photo-production from the proton were used. For the missing

neutron momentum greater than 0.18 GeV/c, the generated events were weighted by $\frac{d\sigma}{dP_n d\Omega_n d\Omega_p}$ from Ref.[10] to include both the $\phi - N$ and $N - N$ final state interactions. In both cases, the ϕ mass distribution was modeled by a Breit-Wigner shape with the resonance centered at the ϕ mass of 1.019 GeV/c² and with a FWHM of 0.0044 GeV/c². The ϕ -meson decay angular distribution was taken as [19]:

$$W(\cos(\theta_H)) = \frac{3}{2} \left(\frac{1}{2} (1 - \rho_{00}^0) \sin^2 \theta_H + \rho_{00}^0 \cos^2 \theta_H \right) + \alpha \cos \theta_H, \quad (2)$$

where ρ_{00}^0 is the spin density matrix element, θ_H denotes the polar angle of the K^+ in the ϕ -meson rest frame, and α accounts for an interference between the ϕ and the non-resonant S -wave K^+K^- pair production [20]. Helicity conserving amplitudes give $\rho_{00}^0 = 0$, while single-helicity flip amplitudes require $\rho_{00}^0 \neq 0$. A value of 0.1 (0.05) was used for ρ_{00}^0 (α) in the MC simulation. The MC generated events were used as input to the GEANT3-based CLAS simulation [16]. They were then reconstructed using the same event reconstruction algorithm as was used for the data. The acceptance was obtained by the ratio of the number of events that passed the analysis cuts to the number of generated ϕ events. The average differential cross section for each photon energy and $|t - t_0|$ bin was extracted by dividing the normalized yield (number of selected events divided by the integrated photon flux including the DAQ dead time, the target thickness, the ϕ decay branching ratio and $|t - t_0|$ bin size) by the acceptance which includes the detection efficiency. The differential cross sections were then bin-centered at fixed t values and a finite binning correction was applied.

Several sources contribute to the overall systematic uncertainty in extracting the differential cross section. The systematic uncertainties associated with particle identification and the missing mass cut were determined to be 0.5 - 7.0% and 0.5 - 5.0%, which are the values found across the different bins of photon energy and t , respectively. These were determined by varying the corresponding cuts by $\pm 10\%$. The uncertainties in the parameters of the ϕ decay angular distribution, ρ_{00}^0 and α , were 10% and 5% [18, 20], respectively, leading to 1.5-6.5% systematic uncertainties. The background obtained from the non-linear background shape was on average 5% smaller than that from the linear background. The systematic uncertainties from the acceptance dependence on the cross section model varied from 0.5% to 9%. The uncertainty in the photon flux was 5% [21, 22]. The uncertainty of the bin-centering corrections were typically between 0.5% and 6.0%, based on our current knowledge of the CLAS detector and the uncertainty in the input cross section. Combining all systematic uncertainties in quadrature, the overall systematic uncertainties vary from 7% - 18% depending on the kinematics.

In Fig. 2, differential cross sections, $\frac{d\sigma}{dt}$ from this work

(red solid circles) for the reaction $\gamma + d \rightarrow \phi + p + n$ are presented. In Fig. 2a and Fig. 2b, we present $\frac{d\sigma}{dt}$ as a function of $|t - t_0|$ for a photon energy range of 1.65 - 2.62 GeV and 2.62 - 3.59 GeV, respectively (same as those in Ref.[13]). The detected proton and the missing neutron momentum span a range of 0.18 to 2.0 GeV/c (Figs. 2a and 2b). For the low missing momentum region (the momenta of the reconstructed neutron smaller than 0.18 GeV/c), cross sections over the same photon energy ranges are shown in Fig. 2c and Fig. 2d. The error bars shown are the statistical uncertainties, and the overall systematic uncertainties are shown by the black band. Also plotted are the predictions [10] for quasi-free ϕ production and rescattering for four sets of $\sigma_{\phi N}$ and $\beta_{\phi N}$. The calculations are performed based on the model assumptions of pomeron exchange or the two-gluon exchange interaction in the $\phi - N$ rescattering process.

In [10], the neutron-proton rescattering amplitude has been taken into account and treated in the same way as in the analysis of the $d(e, e'p)n$ channel [23, 24]. The models for the ϕ photoproduction on the proton [25, 26] used in Ref. [10] describe the published experimental cross sections [20, 27] reasonably well for photon energies in the vicinity of 3.4 GeV and above. However, at low photon

energies the model underestimates the experimental cross sections of $\gamma + p \rightarrow \phi + p$ [18] above $|t - t_0| = 1$ (GeV/c)² by a factor that can reach 10 at 2.5 (GeV/c)². The extracted cross sections [28] of the $\gamma + "p" \rightarrow p + \phi$ from the $d(\gamma, \phi p)n$ channel at low neutron missing momentum from this work are in good agreement with the extracted cross sections of $\gamma + p \rightarrow \phi + p$ [18]. The flattening behavior of the experimental cross sections with increasing $|t - t_0|$ values is well accounted for by the coupling between the ϕ and ω production channels [29], which is discussed later. This channel coupling effect has not yet been implemented in Laget's code that we use, and its effect will be investigated in a future study.

We simply note that in the high missing momentum region where contributions of rescattering processes ($\phi - N$ or $N - N$) are significant, the dominant contribution to the matrix element comes from the photoproduction of ϕ on a nucleon at rest, which gets its measured momentum in the rescattering process (we refer to Ref. [10] for a detailed discussion). The consequence is that in the scattering loop the elementary photoproduction amplitude $\gamma + N \rightarrow \phi + N$ is almost the same as in the quasifree case, when the spectator is at rest. The amplitude for the $\gamma + d \rightarrow \phi + p + n$ process can be written as:

$$A = A_{\phi p}^{QS} \otimes (1 + A_{pn}^{f si} + A_{\phi n}^{f si}) + A_{\phi n}^{QS} \otimes (1 + A_{pn}^{f si} + A_{\phi p}^{f si}) = (A_{\phi p}^{QS} + A_{\phi n}^{QS}) \otimes (1 + A_{pn}^{f si} + A_{\phi N}^{f si}) \quad (3)$$

where $A_{\phi N}^{QS}$, $A_{pn}^{f si}$ and $A_{\phi N}^{f si}$ are the amplitude for the ϕ -meson photoproduction from nucleon, the amplitude for the proton-neutron final state interaction, and the amplitude for the ϕ -N final state interaction, respectively. The second step assumes isospin symmetry for the ϕ -N interaction. The \otimes represents a convoluted integral over internal momentum. Thus, deviations from data in the model cross section of ϕ photoproduction from nucleons will lead to deviations of the calculated cross sections in the high spectator nucleon momentum region from the data, even without final state interaction effects. In order to minimize this effect, we form the following ratio between the results with a high spectator momentum cut and the results with a low spectator momentum cut for each value of $|t - t_0|$:

$$R = \frac{\sigma_H}{\sigma_L} = \frac{\int_{0.18\text{GeV}}^{2\text{GeV}} \frac{d\sigma}{dt dP_{miss}} \cdot dP_{miss}}{\int_{0.1\text{GeV}}^{0.18\text{GeV}} \frac{d\sigma}{dt dP_{miss}} \cdot dP_{miss}} \quad (4)$$

The amplitude with a low spectator nucleon momentum cut is

$$A = A_{\phi p}^{QS} + A_{\phi n}^{QS} \quad (5)$$

within the quasi-free reaction mechanism. Therefore, the

extracted ratio is

$$R \sim \frac{|(A_{\phi p}^{QS} + A_{\phi n}^{QS}) \otimes (1 + A_{pn}^{f si} + A_{\phi N}^{f si})|^2}{|(A_{\phi p}^{QS} + A_{\phi n}^{QS})|^2} \quad (6)$$

$$\sim |(1 + A_{pn}^{f si} + A_{\phi N}^{f si})|^2$$

The second step relies on the factorization approximation which works better when the elementary amplitude varies slowly with energy. This is the case for the ϕ -meson photoproduction channel. This implies that to first order in the ratio R , the elementary ϕ photoproduction amplitude and, hence, the related model uncertainties, should cancel out.

The comparison of the experimental ratios to the model calculations from Ref.[10] are presented in Fig. 3. The experimental data are shown with statistical uncertainties. The systematic uncertainties are shown by the black band. In the low energy range, $E_\gamma = 1.65$ -2.62 GeV (Fig. 3a), the data are best described by the parameters of $\sigma_{\phi N} = 10$ mb and $\beta_{\phi N} = 6$ (GeV/c)⁻². In the range $E_\gamma = 2.62$ -3.59 GeV, the data can be described well by all four calculations shown in Fig. 3 including the rescattering effect.

In order to constrain the value of $\sigma_{\phi N}$ using our data,

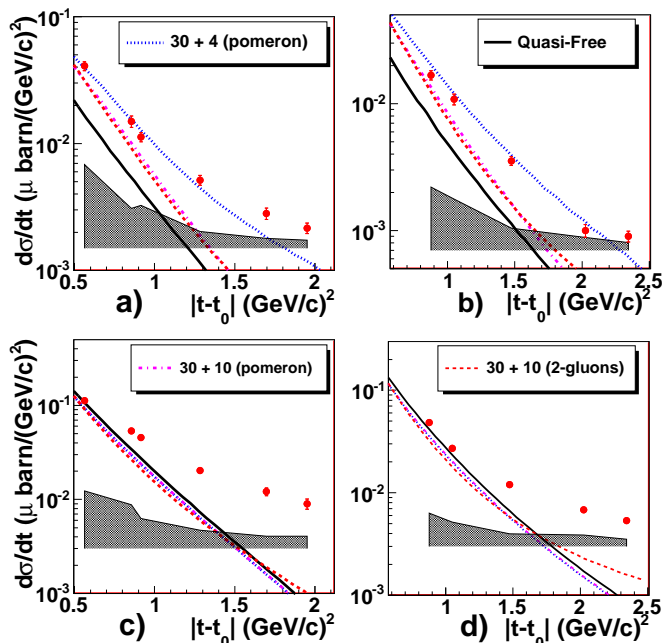


FIG. 2: Differential cross section $\frac{d\sigma}{dt}$ from $\gamma(d, K^+ K^- p)n$ process for photon energies of 1.65-2.62 GeV (a, c) and 2.62-3.59 GeV (b, d). The missing momentum is higher than 0.18 GeV/c in (a) and (b), and lower than 0.18 GeV/c in (c) and (d). The results of this work are shown in red solid circles. The black bands represent the systematic uncertainties. The label “30 + 10” indicates the calculation from Laget [10] with $\sigma_{tot}^{\phi N} = 30$ mb and $\beta_{\phi N} = 10$ (GeV/c) $^{-2}$. The legend for the calculations is presented for better visibility and it applies to all four panels.

a χ^2 analysis was performed for results from both the $\gamma + d \rightarrow \phi + p + (n)$ process ($R = \frac{\sigma_H}{\sigma_L}$) and the published $\gamma + d \rightarrow \phi + d$ coherent channel [13] by mapping the phase space of $\sigma_{\phi N}$ and $\beta_{\phi N}$. The χ^2 is defined as:

$$\chi^2 = \sum_{i=1}^N \frac{(R_{data} - R_{cal})^2}{\delta R_{data}^2}, \quad (7)$$

where N is the number of data points. R_{data} (R_{cal}) is the cross section ratio defined in Eq. 3 for data (calculation). The δR_{data} is quadrature sum of the point-to-point systematic uncertainty and the statistical uncertainty. For the coherent process, R_{data} (R_{cal}) is the differential cross section data (calculation). The calculations of Laget [10], which include pomeron exchange for the elementary ϕ meson photoproduction cross section on the nucleon, are used for the $\gamma + d \rightarrow \phi + p + n$ channel. The pomeron and the two-gluon exchange versions of the model lead to very similar results at $|t - t_0|$ values smaller than 1.5 (GeV/c) 2 , as can be seen in Fig. 2 and Fig. 3. For the coherent production channel, calculations from Sargsian *et al.* [11, 12] are used.

Fig. 4a and Fig. 4b show the confidence level for both

processes in the two photon energy regions. While the energy dependence in $\sigma_{\phi N}$ and $\beta_{\phi N}$ might be a possible explanation for the difference between Fig. 4a and 4b, the combined analysis favors a value of $\sigma_{\phi N}$ larger than 20 mb. Our results are consistent with that extracted from the SPring-8 data [6] in which Li, C, Al and Cu nuclear targets were used. Further more, our combined analysis gives a lower bound of 6 (GeV/c) $^{-2}$ for the $\beta_{\phi N}$ parameter.

Medium modifications that have been suggested by the SPring-8 data [6] can hardly explain a large $\sigma_{\phi N}$ cross section (large r_ϕ) in deuterium. More likely it may reflect the fact that other mechanisms, beyond np and ϕN rescattering, are at play and are more important than the medium modifications, for example the QCD van der Waals force. On the one hand, the coupling of the ϕ (via two-gluon exchange) to hidden color components [30] inside the deuteron may contribute to large missing momenta and leave less room for $\phi - N$ rescattering. On the other hand, the coupling to a cryptoexotic baryon (baryon with hidden strangeness), $B_\phi = udds\bar{s}$, may also contribute [2]. However, the most likely explanation lies in the $\omega - \phi$ mixing. The photon produces an ω meson on one nucleon, which elastically scatters on the second nucleon before transforming into a ϕ meson. The corresponding matrix element has the same structure as the elastic ϕ rescattering matrix element that we considered in our analysis. An effective $\sigma_{\phi N}$ cross section value can be written as:

$$\sigma_{\phi N}^{eff} \sim \sigma_{\phi N} + \sigma_{\omega N} \sqrt{\frac{\sigma_{\gamma N \rightarrow \omega N}}{\sigma_{\gamma N \rightarrow \phi N}}} g_{\omega \rightarrow \phi}. \quad (8)$$

With the experimental value of $\frac{\sigma_{\gamma N \rightarrow \omega N}}{\sigma_{\gamma N \rightarrow \phi N}} \sim 50$ [27, 31] in a $-t$ region of 1 to 3 (GeV/c) 2 , and the $\omega - \phi$ mixing coefficient $g_{\omega \rightarrow \phi} \sim 0.09$ [32], one can reconcile the effective ϕN cross section of ~ 30 mb with the VMD values of the $\sigma_{\omega N}$ (~ 25 mb) and $\sigma_{\phi N}$ (~ 10 mb) [29]. One way to put the $\phi - N$ cross section on more solid ground would be to select the part of the phase space where the $\phi - N$ rescattering dominates, using the method proposed in Ref. [10]. Future high statistics data from a luminosity upgraded CLAS12 [33] detector will help disentangle these possibilities. Furthermore, future improved and new theoretical calculations will allow us to study the model uncertainty in the extraction of the $\phi - N$ total cross section.

We thank Misak Sargsian and Mark Strikman for helpful conversations. We acknowledge the outstanding efforts of the staff of the Accelerator and Physics Divisions at Jefferson Lab who made this experiment possible. This work was supported in part by the U.S. Department of Energy under contract number DE-FG02-03ER41231, the National Science Foundation, the Istituto Nazionale di Fisica Nucleare, the French Centre National de la Recherche Scientifique, the French Commissariat à l’Energie Atomique, the U.S. Department of

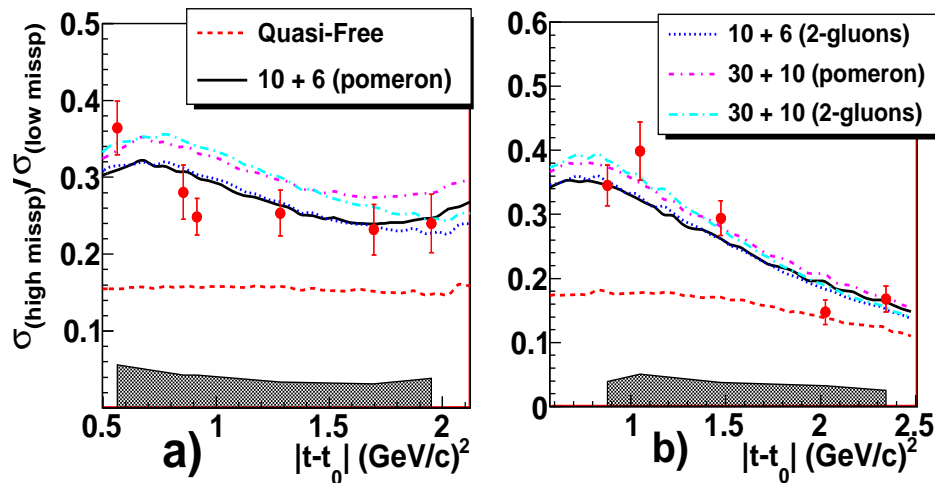


FIG. 3: Cross section ratio between the high and the low missing momentum regions for photon energies of 1.65-2.62 GeV (a) and 2.62-3.59 GeV (b). The results of this work are shown in red solid circles. The black bands represent the systematic uncertainties. We use same notations as those in Fig. 2 for calculations from Laget [10].

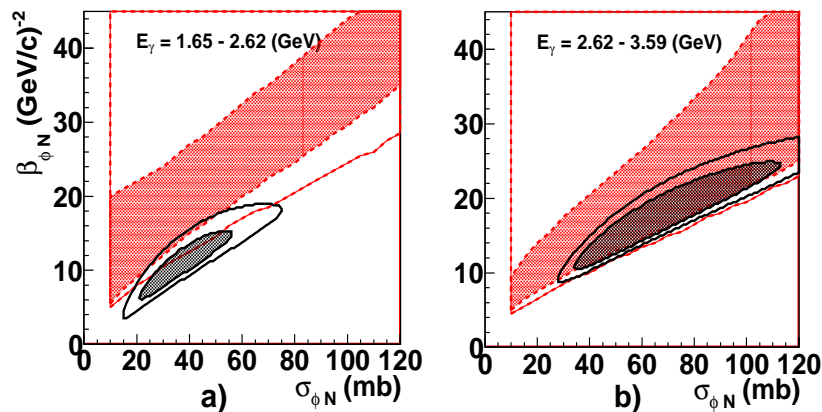


FIG. 4: The 70% (shaded area) and the 95% (open area) confidence level plots shown for the $\gamma + d \rightarrow \phi + p + (n)$ channel (red), the $\gamma + d \rightarrow \phi + d$ coherent channel (black) for photon energies of 1.65-2.62 GeV (a) and 2.62-3.59 GeV (b).

Energy, the National Science Foundation, the UK Science and Technology Facilities Council (STFC), and the Korean Science and Engineering Foundation. The South-eastern Universities Research Association (SURA) operates the Thomas Jefferson National Accelerator Facility for the United States Department of Energy under contract DE-AC05-84ER40150.

* Current address: University of Kentucky, Lexington, KY 40506

† Current address: Thomas Jefferson National Accelerator Facility, Newport News, VA 23606

‡ Current address: Los Alamos National Laboratory, New

Mexico, NM 87545

§ Current address: The George Washington University, Washington, DC 20052

¶ Current address: Edinburgh University, Edinburgh EH9 3JZ, United Kingdom

** Current address: College of William and Mary, Williamsburg, VA 23187

- [1] S. J. Brodsky, I. A. Schmidt and G. F. de Teramond, Phys. Rev. Lett. **64**, 1011 (1990).
- [2] A. Sibirtsev *et al.*, Eur. Phys. J. **A29**, 209 (2006).
- [3] J. J. Sakurai, Currents and Mesons, University of Chicago Press, Chicago, 1969.
- [4] H. J. Lipkin, Phys. Rev. Lett. **16**, 1015 (1966).
- [5] B. Povh and J. Hüfner, Phys. Rev. Lett. **58**, 1612 (1987).
- [6] T. Ishikawa *et al.*, Phys. Lett. **B608**, 215 (2005).
- [7] G.E. Brown and M. Rho, Phys. Rev. Lett. **66**, 2720 (1991).

- [8] L. L. Frankfurt and M. I. Strikman, Nucl. Phys. **B250**, 143 (1985); L. L. Frankfurt and M. I. Strikman, Phys. Rep. **160**, 235 (1988).
- [9] G.R. Farrar, L.L. Frankfurt, M.I. Strikman and H. Liu, Phys. Rev. Lett. **64**, 2996 (1990).
- [10] J-M. Laget, Phys. Rev. **C73**, 044003 (2006).
- [11] L. Frankfurt *et al.*, Nucl. Phys. **A622**, 511 (1997).
- [12] T. C. Rogers, M. M. Sargsian, and M. I. Strikman, Phys. Rev. **C56**, 1124 (1997).
- [13] T. Mibe *et al.*, Phys. Rev. C **76**, 052202R (2007).
- [14] D.I. Sober *et al.*, Nucl. Instrum. Methods A **440**, 263 (2000).
- [15] B.A. Mecking *et al.*, Nucl. Instrum. Methods A **503**, 513 (2003).
- [16] http://www.physics.unh.edu/maurik/gsim_info.shtml.
- [17] R. Machleidt, K. Holinde, and C. Elster, Phys. Rep. **149**, 1 (1987).
- [18] D. Tedeschi *et al.* (CLAS Collaboration), to be submitted.
- [19] K. Schilling, P. Seyboth, and G. E. Wolf, Nucl. Phys. **B15**, 397 (1970).
- [20] K. McCormick *et al.*, Phys. Rev. C **69**, 032203 (2004).
- [21] J. Ball and E. Pasyuk, CLAS-NOTE **2005-002** (2005), <http://www.jlab.org/ul/Physics/Hall-B/clas/public/2005-002.pdf>.
- [22] W. Chen *et al.* (CLAS Collaboration), Phys. Rev. Lett. **103**, 012301 (2009), arXiv:0903.1260 (nucl-ex).
- [23] J-M. Laget, Phys. Lett. **B609**, 49 (2005).
- [24] K. Egiyan *et al.*, Phys. Rev. Lett. **98**, 262502 (2007).
- [25] J-M. Laget, Phys. Lett. **B489**, 313 (2000)
- [26] F. Cano and J-M. Laget, Phys. Rev. **D65**, 074022. (2002).
- [27] E. Anciant *et al.*, Phys. Rev. Lett. **85**, 4682 (2000).
- [28] X. Qian *et al.*, to be submitted.
- [29] J.-M. Laget *et al.*, to be published.
- [30] J-M. Laget and R. Mendez-Galain, Nucl. Phys. **A581**, 397 (1995).
- [31] M. Battaglieri *et al.* (CLAS Collaboration), Phys. Rev. Lett. **90**, 022002 (2003).
- [32] Particle Data Group: C. Amsler *et al.*, Phys. Lett. B **667**, 1 (2008).
- [33] <http://www.jlab.org/Hall-B/clas12/>